Hindawi Publishing Corporation
Boundary Value Problems
Volume 2010, Article ID 731741, 13 pages
doi:10.1155/2010/731741

Research Article

Image Location for Screw Dislocation—A New Point of View

Jeng-Tzong Chen,[1,2] Ying-Te Lee,[1] Ke-Hsun Chou,[1] and Jia-Wei Lee[1]

[1] *Department of Harbor and River Engineering, National Taiwan Ocean University, Keelung 20224, Taiwan*
[2] *Department of Mechanical and Mechatronic Engineering, National Taiwan Ocean University, Keelung 20224, Taiwan*

Correspondence should be addressed to Jeng-Tzong Chen, jtchen@mail.ntou.edu.tw

Received 16 June 2009; Accepted 18 January 2010

Academic Editor: Colin Rogers

An infinite plane problem with a circular boundary under the screw dislocation is solved by using a new method. The angle-based fundamental solution for screw dislocation is expanded into degenerate kernel. Our method can explain why the image screw dislocation is required. Besides, the location of the image point can be obtained easily by using degenerate kernel after satisfying boundary conditions. Even though the image concept is required, the location of image point can be determined straightforwardly through the degenerate kernel instead of the method of reciprocal radii. Finally, two examples are demonstrated to verify the validity of the present method.

1. Introduction

The dislocation theory is essential for understanding many physical and mechanical properties of crystalline solids. Many researchers investigated the dislocation problems in the past years. Smith [1] successfully solved the problem of the interaction between a screw dislocation and a circular or elliptic inclusion contained within an infinite body subject to a uniform applied shear stress at infinity by using the complex-variable function and circle theorem. Dundurs [2] solved the screw dislocation with circular inclusion problem by using the image technique. Later, Sendeckyj [3] employed the complex-variable function in conjunction with the inverse point method to solve the problem of the screw dislocation near an arbitrary number of circular inclusions. Almost all above problems were solved by using the complex-variable technique. Its extension to three-dimensional cases may be limited. A more general approach is nontrivial for further investigation.

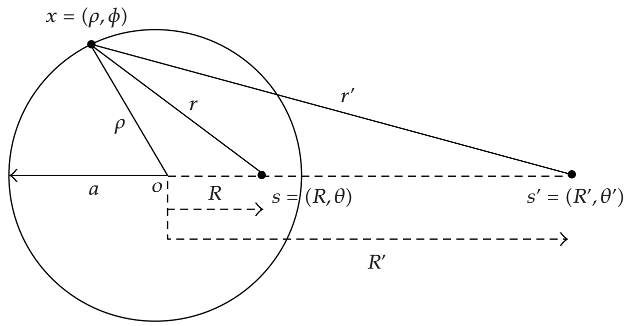

Figure 1: Method of reciprocal radii.

In the potential theory, it is well known that the image method can solve potential problems when the fundamental solution is known. The image point was found in a semi-inverse method a priori through the reciprocal radii in the Sommerfeld's book [4] as shown in Figure 1. Sommerfeld and Greenberg [5] both utilized the concept of reciprocal radii of Thomson [6] to derive the Poisson integral formula. It is important to find where the location of image point is. However, we do not find a natural and logical way about how to determine the location of image point in the literature until an alternative way proposed by Chen and Wu [7]. Chen and Wu derived the location of image point for a source singularity in a straightforward way through the use of degenerate kernel and proved an alterative way to derive the Poisson integral formula. The fundamental solutions of source singularity are expanded into degenerate kernels for constructing the Green's function. Since the degenerate kernel separates the source and field points for the closed-form fundamental solution, it plays an important role in studying the image location [8, 9]. To determine the location of image point for screw dislocation in a straightforward way is the main concern of the present paper.

In this paper, we will introduce the degenerate (or so-called separable) kernel for the angle-based fundamental solution (ψ) for the screw dislocation instead of radial-basis one ($\ln r$) for the source singularity. By employing the degenerate kernel, the closed-form Green's function is expanded into the degenerate form. Also, the location of image point is found in a straightforward way. The two-dimensional Laplace exterior problems are solved. Finally, two examples were given to demonstrate the validity of the present method.

2. Degenerate (Separable) Kernel for the Angle-Based Fundamental Solution

It is well known that the fundamental solution of two-dimension Laplace problem with a concentrated source is $\ln(r)$, where r is the distance between the field point x and the source point s as shown in Figure 2. The strength of the fundamental solution is -2π instead of unity. Here, we give the screw dislocation to replace the concentrated source and then the angle-based fundamental solution ψ is used to substitute the radial-based one as shown in Figure 2. In order to fully capture circular geometry, we utilize the polar coordinates to replace the Cartesian coordinates. Therefore, the location of the screw dislocation s and the position of field point x are expressed as (R, θ) and (ρ, ϕ), respectively, in the polar coordinate system. The position vector of screw dislocation point s can be written as complex form, $z_s = Re^{i\theta}$.

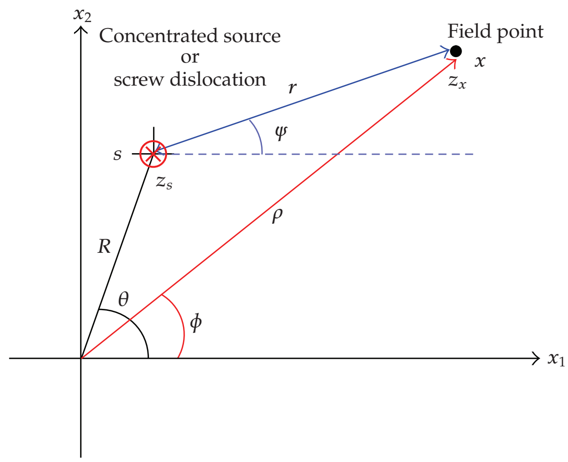

Figure 2: Sketch of the concentrated source and the screw dislocation.

Similarly, the field point x can be expressed by $z_x = \rho e^{i\phi}$ in the complex plane as shown in Figure 2. By decomposing the $\ln(z_x - z_s)$ into real and imaginary parts, we have

$$\ln(z_x - z_s) = \ln\left(re^{i\psi}\right) = \ln r + i\psi. \tag{2.1}$$

The real part ($\ln r$) is the fundamental solution of the source singularity while the imaginary part (ψ) denotes the fundamental solution of the screw dislocation. For the exterior case ($R < \rho$), (2.1) can be expanded as follows:

$$\begin{aligned}
\ln(z_x - z_s) &= \ln(z_x) + \ln\left(1 - \frac{z_s}{z_x}\right) \\
&= \ln\left(\rho e^{i\phi}\right) - \sum_{m=1}^{\infty} \frac{1}{m}\left(\frac{z_s}{z_x}\right)^m \\
&= \ln\rho + i\phi - \sum_{m=1}^{\infty} \frac{1}{m}\left(\frac{Re^{i\theta}}{\rho e^{i\phi}}\right)^m \\
&= \ln\rho + i\phi - \sum_{m=1}^{\infty} \frac{1}{m}\left(\frac{R}{\rho}\right)^m \left[\cos m(\theta-\phi) + i\sin m(\theta-\phi)\right].
\end{aligned} \tag{2.2}$$

Thus, the degenerate form for the fundamental solution of the screw dislocation, $\psi(s, x)$, can be expressed as

$$\psi(s, x) = \phi - \sum_{m=1}^{\infty} \frac{1}{m}\left(\frac{R}{\rho}\right)^m \sin m(\theta - \phi), \quad \rho > R. \tag{2.3}$$

Similarly, we have

$$\psi(s,x) = \theta + \pi + \sum_{m=1}^{\infty} \frac{1}{m}\left(\frac{\rho}{R}\right)^m \sin m(\theta - \phi), \quad \rho < R, \tag{2.4}$$

for the interior case. In Figure 2, the range of $\psi(s,x)$ is defined between 0 and 2π. To match the physical meaning and mathematical requirement, we modify the range of interest between $-\pi$ and π. Thus, the fundamental solution of the screw dislocation $\psi(s,x)$ is expressed by

$$\psi(s,x) = \begin{cases} \psi^I(R,\theta;\rho,\phi) = \theta + \displaystyle\sum_{m=1}^{\infty} \frac{1}{m}\left(\frac{\rho}{R}\right)^m \sin m(\theta - \phi), & \rho < R, \\ \psi^E(R,\theta;\rho,\phi) = \phi - \pi - \displaystyle\sum_{m=1}^{\infty} \frac{1}{m}\left(\frac{R}{\rho}\right)^m \sin m(\theta - \phi), & \rho > R, \end{cases} \tag{2.5}$$

where the superscripts I and E denote the interior and exterior cases, respectively. It is noted that the denominator in (2.5) involves the larger argument to ensure the series convergence. The displacement contour of the screw dislocation in the four quadrants by using (2.5) is shown in Figures 3(a)–3(d). When the screw dislocation locates at the four quadrants, there are certain areas falling outside the range between $-\pi$ and π. We subtract 2π, where the value is greater than π to ensure the value in the range. Similarly, we add 2π, where the value is smaller than $-\pi$. When the response falls in the defined range, Figure 4 shows the displacement contour for the screw dislocation. To the authors' best knowledge, the degenerate kernel for the angle-based fundamental solution was not found in the literature.

3. 2D Exterior Problem

For the problem of an infinite plane problem with a circular boundary under the screw dislocation as shown in Figure 5(a), the function of displacement field satisfies

$$\begin{gathered} \nabla^2 U_G(x) = 0, \quad x \in \Omega, \\ U_G(\rho,\phi)\,|_{\phi=2\pi} - U_G(\rho,\phi)\,|_{\phi=0} = b, \quad \rho > R, \end{gathered} \tag{3.1}$$

where Ω is the domain of interest and b is the Burger's vector which is equal to 2π in this paper. The boundary condition on the circular boundary is the Dirichlet type

$$U_G(x)|_{x\in B} = U_G(\rho,\phi)\,|_{\rho=a} = 0, \tag{3.2}$$

where a is the radius of the circular boundary and B is the circular boundary. By employing the image method, the image point is located outside the domain and the solution can be represented as follows:

$$U_G(x;s,s') = \psi(s,x) + \psi(s',x) + c, \tag{3.3}$$

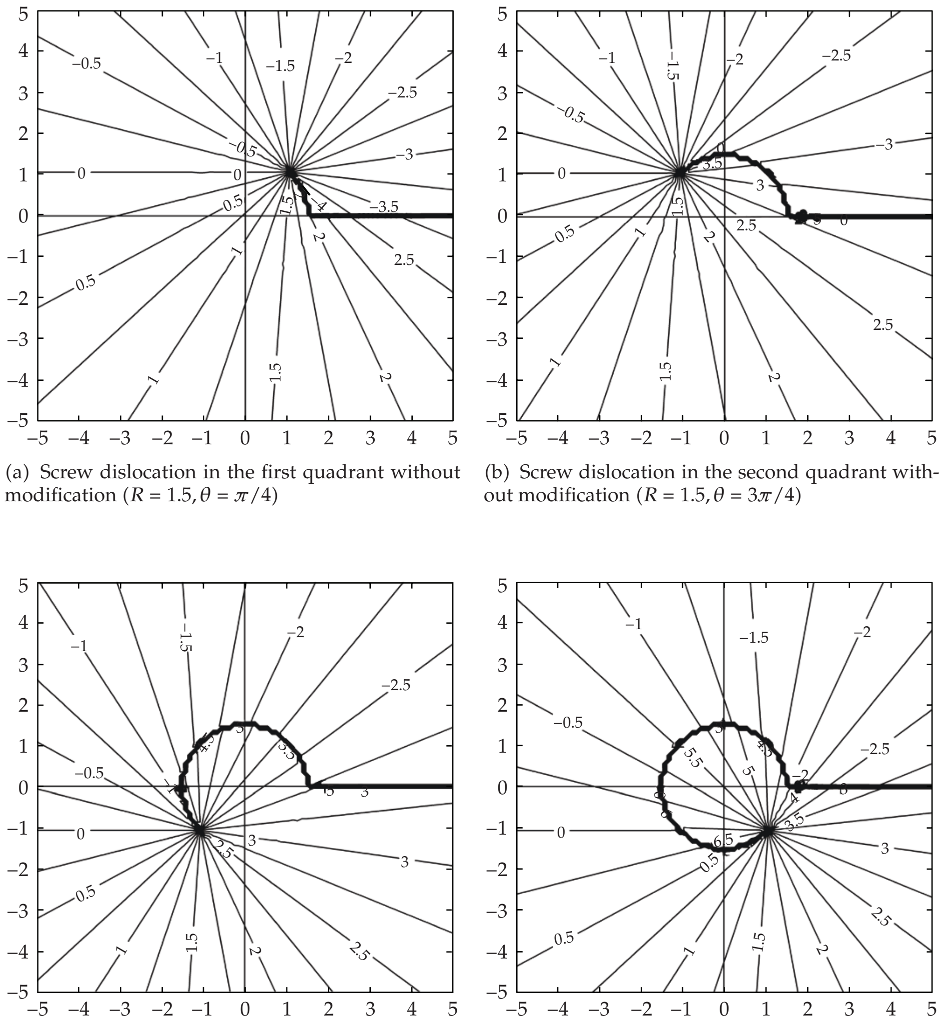

(a) Screw dislocation in the first quadrant without modification ($R = 1.5, \theta = \pi/4$)

(b) Screw dislocation in the second quadrant without modification ($R = 1.5, \theta = 3\pi/4$)

(c) Screw dislocation in the third quadrant without modification ($R = 1.5, \theta = 5\pi/4$)

(d) Screw dislocation in the forth quadrant without modification ($R = 1.5, \theta = 7\pi/4$)

Figure 3: Screw dislocation in (a) the first, (b) the second, (c) the third, and (d) the forth quadrant without modification.

where s' is the location of image point, c is a free constant, and

$$\begin{aligned}\psi(s,x) &= \theta + \sum_{m=1}^{\infty} \frac{1}{m}\left(\frac{\rho}{R}\right)^{m} \sin m(\theta - \phi), \quad \rho < R,\\ \psi(s',x) &= \phi - \pi - \sum_{m=1}^{\infty} \frac{1}{m}\left(\frac{R'}{\rho}\right)^{m} \sin m(\theta' - \phi), \quad \rho > R'.\end{aligned} \tag{3.4}$$

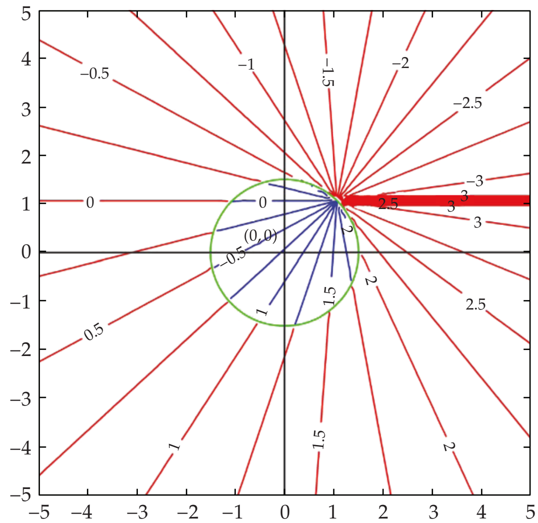

Figure 4: Screw dislocation in the first quadrant after modification ($R = 1.5$, $\theta = \pi/4$).

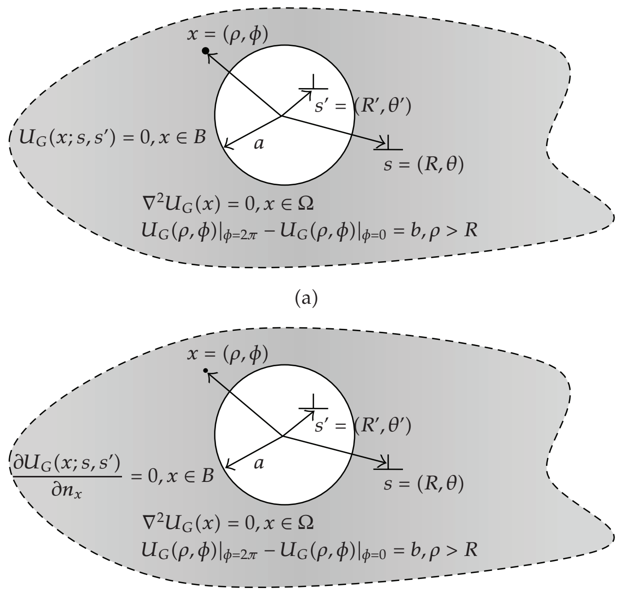

Figure 5: 2D exterior problem (a) Dirichlet boundary condition and (b) Neumann boundary condition.

In order to match the boundary condition and the Burger's vector, first the sum of series is independent of ϕ. Therefore, we choose the collinear points s and s', that is, $\theta = \theta'$ and we have

$$\sum_{m=1}^{\infty} \frac{1}{m}\left(\frac{a}{R}\right)^m \sin m(\theta - \phi) - \sum_{m=1}^{\infty} \frac{1}{m}\left(\frac{R'}{a}\right)^m \sin m(\theta - \phi) = 0. \tag{3.5}$$

Finally, we can obtain the location of image point

$$\frac{R'}{a} = \frac{a}{R} \Longrightarrow R' = \frac{\rho^2}{R} = \frac{a^2}{R}, \tag{3.6}$$

$$\psi(s,x) + \psi(s',x) = \theta + \phi - \pi. \tag{3.7}$$

Second, we found that c is equal to $(-\theta - \phi + \pi)$ and the solution $U_G(x; s, s')$ automatically matches the boundary condition and Burger's vector. The displacement field of the closed-form Green's function can be obtained as below

$$U_G(x; s, s') = \psi(s,x) + \psi(s',x) - \theta - \phi + \pi. \tag{3.8}$$

For the domain $(a < \rho < R)$ as shown in Figure 6(a), the Green's function is expanded into

$$\begin{aligned} U_G(x; s, s') &= \psi(s,x) + \psi(s',x) - \theta - \phi + \pi \\ &= \theta + \sum_{m=1}^{\infty} \frac{1}{m}\left(\frac{\rho}{R}\right)^m \sin m(\theta - \phi) \\ &\quad + \phi - \pi - \sum_{m=1}^{\infty} \frac{1}{m}\left(\frac{a^2}{\rho R}\right)^m \sin m(\theta - \phi) - \theta - \phi + \pi \\ &= \sum_{m=1}^{\infty} \frac{1}{m}\left[\left(\frac{\rho}{R}\right)^m - \left(\frac{a^2}{\rho R}\right)^m\right] \sin m(\theta - \phi), \quad a < \rho < R. \end{aligned} \tag{3.9}$$

Similarly, the Green's function in the other region $(R < \rho < \infty)$ is shown in Figure 6(b) and is expanded into

$$\begin{aligned} U_G(x; s, s') &= \psi(s,x) + \psi(s',x) - \theta - \phi + \pi \\ &= \phi - \pi - \sum_{m=1}^{\infty} \frac{1}{m}\left(\frac{R}{\rho}\right)^m \sin m(\theta - \phi) \\ &\quad + \phi - \pi - \sum_{m=1}^{\infty} \frac{1}{m}\left(\frac{a^2}{\rho R}\right)^m \sin m(\theta - \phi) - \theta - \phi + \pi \\ &= \phi - \theta - \pi - \sum_{m=1}^{\infty} \frac{1}{m}\left[\left(\frac{R}{\rho}\right)^m + \left(\frac{a^2}{\rho R}\right)^m\right] \sin m(\theta - \phi), \quad R < \rho < \infty. \end{aligned} \tag{3.10}$$

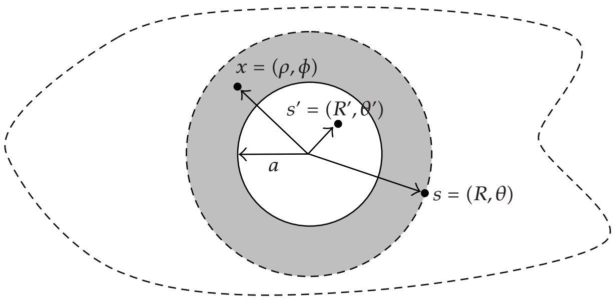

(a)

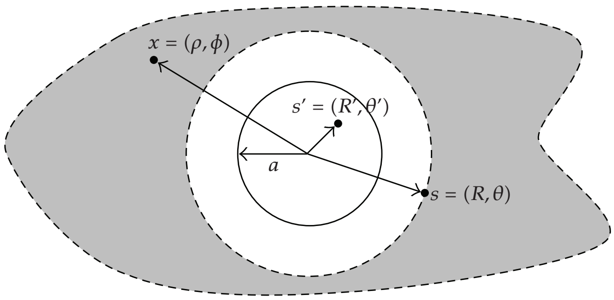

(b)

Figure 6: Green's function of (a) the inner domain ($a < \rho < R$) and (b) the outer domain ($R < \rho < \infty$) for the exterior problem.

For comparison, the closed-form solution of Smith's solution is expressed in terms of functions of complex variables

$$F(z) = \frac{\mu_E b}{2\pi i}\log(z - z_0) + \frac{\mu_E b}{2\pi i}\log\left(\frac{a^2}{z} - \overline{z}_0\right),$$
$$U_G(x) = \frac{1}{\mu_E}\operatorname{Re}[F(z)], \tag{3.11}$$

where $F(z)$ and μ_E denote the complex function and shear modulus, respectively, $\overline{z}_0$ denotes the conjugate of the position vector of the screw dislocation, and $\operatorname{Re}[\cdot]$ denotes the real part. Figures 7(a) and 7(b) show the contour of displacement field by using the Smith's method [1] and the present approach, respectively. Good agreement is made.

According to the successful experience of the Dirichlet boundary condition for the exterior problem, we extend our approach to the Neumann boundary condition, as shown in Figure 5(b),

$$\left.\frac{\partial U_G(x)}{\partial n_x}\right|_{x\in B} = \left.\frac{\partial U_G(\rho,\phi)}{\partial \rho}\right|_{\rho=a} = 0. \tag{3.12}$$

Table 1: Comparison for the source or sink and the screw dislocation (Dirichlet B. C.).

	Source or sink (Chen and Wu [7])	Screw dislocation (present paper)
$\ln z = \ln r + i\psi$	$\ln r$	ψ
Exterior problem (Dirichlet B. C.)	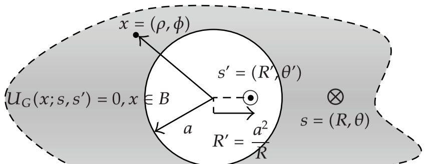 $\nabla^2 U_G(x) = \delta(x - s) - \delta(x - s'), x \in \Omega$	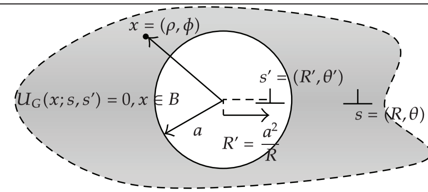 $\nabla^2 U_G(x) = 0, x \in \Omega$ $U_G(\rho, \phi)\|_{\phi=2\pi} - U_G(\rho, \phi)\|_{\phi=0} = b, \rho > R$
The closed form	$U_G(x; s, s') = \ln\|x - s\| - \ln\|x - s'\| + \ln a - \ln R$	$U_G(x; s, s') = \phi(s, x) + \phi(s', x) - \theta - \phi + \pi$
The series form	$U_G(x; s, s') = \begin{cases} \ln\left(\frac{a}{\rho}\right) - \sum_{m=1}^{\infty} \frac{1}{m}\left[\left(\frac{\rho}{R}\right)^m - \left(\frac{a^2}{\rho R}\right)^m\right] \cos m(\theta - \phi), & a < \rho < R \\ \ln\left(\frac{a}{R}\right) - \sum_{m=1}^{\infty} \frac{1}{m}\left[\left(\frac{R}{\rho}\right)^m - \left(\frac{a^2}{\rho R}\right)^m\right] \cos m(\theta - \phi), & R < \rho < \infty \end{cases}$	$U_G(x; s, s') = \begin{cases} \sum_{m=1}^{\infty} \frac{1}{m}\left[\left(\frac{\rho}{R}\right)^m - \left(\frac{a^2}{\rho R}\right)^m\right] \sin m(\theta - \phi), & a < \rho < R \\ \phi - \theta - \pi - \sum_{m=1}^{\infty} \frac{1}{m}\left[\left(\frac{R}{\rho}\right)^m + \left(\frac{a^2}{\rho R}\right)^m\right] \sin m(\theta - \phi), & R < \rho < \infty \end{cases}$
Smith's solution	$\mathrm{F(z)} = \frac{\mu_{\mathrm{E}} \mathrm{b}}{2\pi \mathrm{i}} \log(\mathrm{z} - \mathrm{z}_0) + \frac{\mu_{\mathrm{E}} \mathrm{b}}{2\pi \mathrm{i}} \log\left(\frac{\mathrm{a}^2}{\mathrm{z}} - \bar{\mathrm{z}}_0\right)$ $\mathrm{U_G(x)} = \frac{1}{\mu_{\mathrm{E}}} \mathrm{Im[F(z)]}$	$F(z) = \frac{\mu_E b}{2\pi i} \log(z - z_0) + \frac{\mu_E b}{2\pi i} \log\left(\frac{a^2}{z} - \bar{z}_0\right)$ $U_G(x) = \frac{1}{\mu_E} \mathrm{Re}[F(z)]$

Table 2: Comparison for the source or sink and the screw dislocation (Neumann B.C.).

	Source or sink (Chen and Wu [7])	Screw dislocation (present paper)
$\ln z = \ln r + i\psi$	$\ln r$	ψ
Exterior problem (Neumann B. C.)	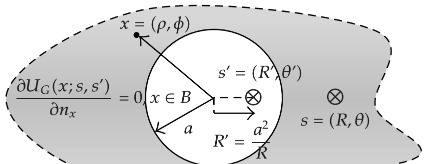 $\nabla^2 U_G(x) = \delta(x-s) - \delta(x-s'), x \in \Omega$	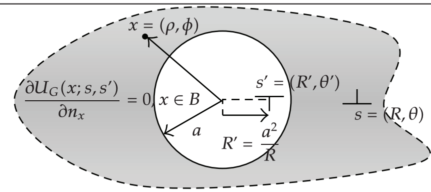 $\nabla^2 U_G(x) = 0, x \in \Omega$ $U_G(\rho,\phi)\vert_{\phi=2\pi} - U_G(\rho,\phi)\vert_{\phi=0} = b, \rho > R$
The closed form	$U_G(x; s, s') = \ln\lvert x-s\rvert + \ln\lvert x-s'\rvert - \ln\rho$	$U_G(x; s, s') = \phi(s, x) - \phi(s', x) + \phi - \pi.$
The series form	$U_G(x; s, s') = \begin{cases} \ln R - \sum_{m=1}^{\infty} \frac{1}{m}\left[\left(\frac{\rho}{R}\right)^m + \left(\frac{a^2}{\rho R}\right)^m\right]\cos m(\theta-\phi), & a < \rho < R \\ \ln\rho - \sum_{m=1}^{\infty} \frac{1}{m}\left[\left(\frac{R}{\rho}\right)^m + \left(\frac{a^2}{\rho R}\right)^m\right]\cos m(\theta-\phi), & R < \rho < \infty \end{cases}$	$U_G(x; s, s') = \begin{cases} \theta + \sum_{m=1}^{\infty} \frac{1}{m}\left[\left(\frac{\rho}{R}\right)^m + \left(\frac{a^2}{\rho R}\right)^m\right]\sin m(\theta-\phi), & a < \rho < R \\ \phi - \pi - \sum_{m=1}^{\infty} \frac{1}{m}\left[\left(\frac{R}{\rho}\right)^m - \left(\frac{a^2}{\rho R}\right)^m\right]\sin m(\theta-\phi), & R < \rho < \infty \end{cases}$
Smith's solution	$F(z) = \frac{\mu_E b}{2\pi i}\log(z-z_0) - \frac{\mu_E b}{2\pi i}\log\left(\frac{a^2}{z} - \bar{z}_0\right)$ $U_G(x) = \frac{1}{\mu_E}\mathrm{Im}[F(z)]$	$F(z) = \frac{\mu_E b}{2\pi i}\log(z-z_0) - \frac{\mu_E b}{2\pi i}\log\left(\frac{a^2}{z} - \bar{z}_0\right)$ $U_G(x) = \frac{1}{\mu_E}\mathrm{Re}[F(z)]$

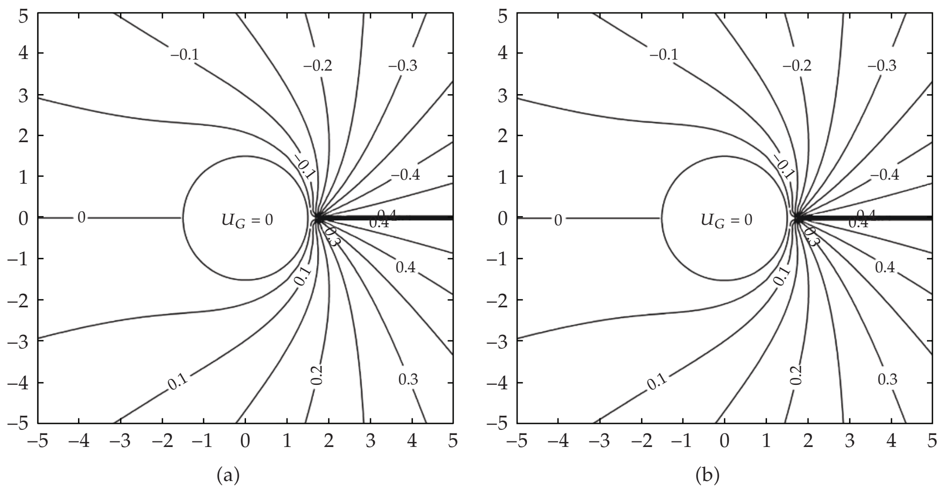

Figure 7: Displacement contour (Dirichlet boundary condition) by using (a) the Smith's method [1] and (b) the present method ($M = 50$).

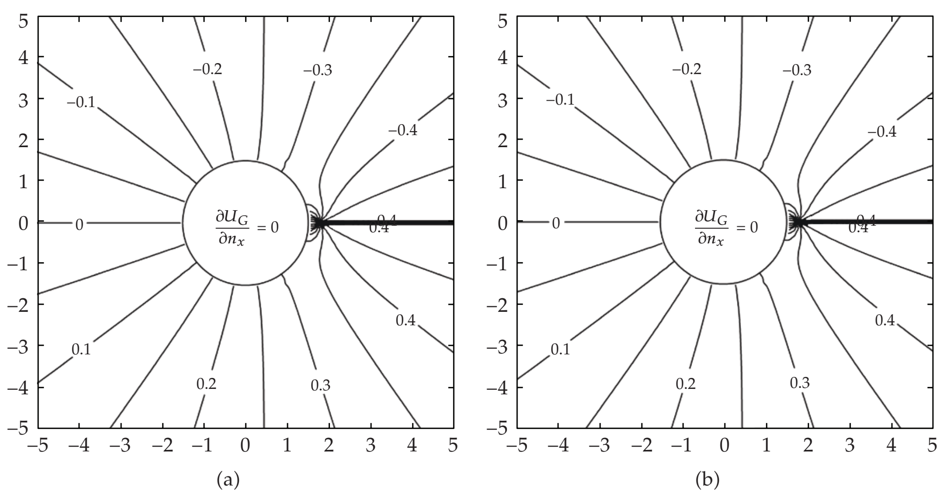

Figure 8: Displacement contour (Neumann boundary condition) by using (a) the Smith's method [1] and (b) the present method ($M = 50$).

In a similar way, we have the closed-form Green's function for the Neumann boundary condition as

$$U_G(x; s, s') = \psi(s, x) - \psi(s', x) + \phi - \pi, \tag{3.13}$$

and the series form is expressed into two parts. For the domain ($a < \rho < R$) as shown in Figure 6(a), the Green's function is expanded into

$$\begin{aligned}
U_G(x;s,s') &= \psi(s,x) - \psi(s',x) + \phi - \pi \\
&= \theta + \sum_{m=1}^{\infty} \frac{1}{m}\left(\frac{\rho}{R}\right)^m \sin m(\theta-\phi) \\
&\quad - \phi + \pi + \sum_{m=1}^{\infty} \frac{1}{m}\left(\frac{a^2}{\rho R}\right)^m \sin m(\theta-\phi) + \phi - \pi \\
&= \theta + \sum_{m=1}^{\infty} \frac{1}{m}\left[\left(\frac{\rho}{R}\right)^m + \left(\frac{a^2}{\rho R}\right)^m\right] \sin m(\theta-\phi), \quad a < \rho < R.
\end{aligned} \tag{3.14}$$

For the other domain as shown in Figure 6(b), we have

$$\begin{aligned}
U_G(x;s,s') &= \psi(s,x) - \psi(s',x) + \phi - \pi \\
&= \phi - \pi - \sum_{m=1}^{\infty} \frac{1}{m}\left(\frac{R}{\rho}\right)^m \sin m(\theta-\phi) \\
&\quad - \phi + \pi + \sum_{m=1}^{\infty} \frac{1}{m}\left(\frac{a^2}{\rho R}\right)^m \sin m(\theta-\phi) + \phi - \pi \\
&= \phi - \pi - \sum_{m=1}^{\infty} \frac{1}{m}\left[\left(\frac{R}{\rho}\right)^m - \left(\frac{a^2}{\rho R}\right)^m\right] \sin m(\theta-\phi), \quad R < \rho < \infty.
\end{aligned} \tag{3.15}$$

For comparison, the closed-form solution of Smith's solution is expressed in terms of functions of complex variable

$$\begin{aligned}
F(z) &= \frac{\mu_E b}{2\pi i}\log(z - z_0) - \frac{\mu_E b}{2\pi i}\log\left(\frac{a^2}{z} - \overline{z}_0\right), \\
U_G(x) &= \frac{1}{\mu_E}\operatorname{Re}[F(z)].
\end{aligned} \tag{3.16}$$

Figures 8(a) and 8(b) show the contour of displacement field by using the Smith's method [1] and the present approach, respectively. It is found that the result of the present approach is acceptable. Based on the image method, it is a straightforward, logical, and natural way to find that the location of image point is (a^2/R). We summarize the result of our approach for the screw dislocation and compare with those of Chen and Wu [7] for the source case in Tables 1 and 2.

4. Conclusions

For the screw dislocation problem with circular boundaries, we have proposed a natural approach to construct the screw dislocation solution by using the degenerate kernel. The angle-based fundamental solution for screw dislocation was derived in terms of degenerate kernel in this paper. Based on this expression, the image location can be determined instead of using reciprocal radius. Two examples, including an infinite plane with a circular hole subject to the Dirichlet and Neumann boundary conditions, were used to demonstrate the validity of the present formulation.

Acknowledgments

The financial support from the National Science Council under Grant no. NSC-98-2221-E-019-017-MY3 for National Taiwan Ocean University is gratefully appreciated. Thanks to Mr. S. R. Yu for preparing the figures.

References

[1] E. Smith, "The interaction between dislocations and inhomogeneities-I," *International Journal of Engineering Science*, vol. 6, no. 3, pp. 129–143, 1968.
[2] J. Dundurs, "Elastic interaction of dislocations with inhomogeneities," in *Mathematical Theory of Dislocations*, T. Mura, Ed., pp. 70–115, American Society of Mechanical Engineers, New York, NY, USA, 1969.
[3] G. P. Sendeckyj, "Screw dislocations near circular inclusions," *Physica Status Solidi*, vol. 30, pp. 529–535, 1970.
[4] A. Sommerfeld, *Partial Differential Equations in Physics*, Academic Press, New York, NY, USA, 1949.
[5] M. D. Greenbreg, *Application of Green's Functions in Science and Engineering*, Prentice-Hill, Upper Saddle River, NJ, USA, 1971.
[6] W. Thomson, *Maxwell in His Treatise*, vol. 1, chapter 11, Oxford University Press, Oxford, UK, 1848.
[7] J. T. Chen and C. S. Wu, "Alternative derivations for the poisson integral formula," *International Journal of Mathematical Education in Science and Technology*, vol. 37, no. 2, pp. 165–185, 2006.
[8] J. T. Chen, H. C. Shieh, Y. T. Lee, and J. W. Lee, "Image solutions for boundary value problems without sources," *Applied Mathematics Computation*, vol. 216, pp. 1453–1468, 2010.
[9] J. T. Chen, Y. T. Lee, S. R. Yu, and S. C. Shieh, "Equivalence between the Trefftz method and the method of fundamental solutions using the addition theorem and image concept," *Engineering Analysis with Boundary Elements*, vol. 33, pp. 678–688, 2009.